Journal Pre-proof

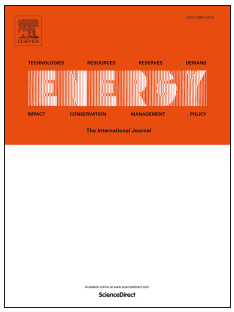

Techno-economic analysis of advanced stripper configurations for post-combustion CO_2 capture amine processes

Hyun-Taek Oh, Youngsan Ju, Kyounghee Chung, Chang-Ha Lee

PII: S0360-5442(20)31271-8

DOI: https://doi.org/10.1016/j.energy.2020.118164

Reference: EGY 118164

To appear in: *Energy*

Received Date: 19 November 2019

Revised Date: 8 June 2020

Accepted Date: 16 June 2020

Please cite this article as: Oh H-T, Ju Y, Chung K, Lee C-H, Techno-economic analysis of advanced stripper configurations for post-combustion CO_2 capture amine processes, *Energy* (2020), doi: https://doi.org/10.1016/j.energy.2020.118164.

Credit Author Statement

Hyun-Taek Oh: Conceptualization, Writing - Original Draft, Writing - Review & Editing, Software, **Youngsan Ju:** Software, **Kyounghee Chung:** Validation, **Chang-Ha Lee:** Writing - Review & Editing, Supervision

Techno-economic analysis of advanced stripper configurations for post-combustion CO_2 capture amine processes

Hyun-Taek Oh, Youngsan Ju, Kyounghee Chung, and Chang-Ha Lee*

Department of Chemical and Biomolecular Engineering, Yonsei University, Seoul, Republic of Korea

*Corresponding author
Tel: +82 2 2123 2762; E-mail: leech@yonsei.ac.kr

Abstract

In chemical absorption processes for carbon capture, one of the main technical challenges is to overcome its high energy requirement for solvent regeneration. A techno-economic analysis was conducted on various modified carbon capture processes using a 30 wt.% monoethanolamine (MEA) solvent. Five configurations of a stripper modified with two or more components of lean vapor compression (LVC), cold solvent split (CSS), and stripper overhead compression (SOC) were designed. Each configuration aimed to reduce the total equivalent work (W_{total}) via heat integration between the condenser and reboiler. The performance was compared with those of conventional and single-modified configurations based on 90% carbon capture from a coal-fired power plant. Compared with the reference results of a pilot plant operation, the thermal energy required from a reboiler could be reduced by 8.1–32.8% through the modified configurations. The developed combined configurations suggested that the W_{total} could be reduced by up to 9.0%, and the operating cost could be saved by up to 10.2%. Although an increase in capital costs is inevitable for process modifications, the advanced configurations can be considered as an alternative to the reference process because energy and operating costs are reduced.

Keywords: Post-combustion CO_2 capture, Techno-economic analysis, monoethanolamine, Advanced process configuration, Process integration

Nomenclature

AMP	2-amino-2-methyl-1 propanol
CAPEX	Capital expenditure
CSS	Cold solvent split
e-NRTL	Electrolyte nonrandom two-liquid
FGD	Flue gas desulfurization
IEA	International energy agency
LVC	Lean vapor compression
MDEA	Methyldiethanolamine
MEA	Monoethanolamine
OPEX	Operational expenditure
PZ	Piperazine
$Q_{thermal}$	Thermal energy
RK	Redlich-Kwong
SIR	Savings-to-Investment ratio
SOC	Stripper overhead compression
T_{sink}	Sink temperature
T_{source}	Source temperature
VLE	Vapor-liquid equilibrium
$W_{electrical}$	Electrical energy
W_{total}	Total equivalent work
$\eta_{turbine}$	Turbine efficiency

1. Introduction

According to the International Energy Agency (IEA), CO_2 emissions from fossil fuel-based electricity production accounted for 40% of the total CO_2 emissions in 2017 [1]. Therefore, technology has been extensively developed to reduce CO_2 emissions from fossil fuel-based power plants. Among notable carbon capture technologies, post-combustion carbon capture technology offers the most significant near-term potential to reduce CO_2 emissions from conventional fossil fuel-based power plants [2].

To capture the carbon emitted from power plants, various capture processes based on dry [3, 4] and wet sorbents [5-7] have been reported. However, the amine-based chemical absorption process is the most successful technology that has been commercialized for many years. Capture processes that use aqueous monoethanolamine (MEA) solvent are a thoroughly researched technology that can be used to treat large volumes of flue gas at atmospheric pressure [8, 9]; these processes are capable of achieving 90% CO_2 capture [10]. Although an amine has rapid reactivity and an excellent absorption capacity [11-13], amine-based chemical capture processes require a high overall operating cost and consume high amounts of regeneration energy [14, 15]. Nevertheless, capture processes that use MEA are widely used as a reference to evaluate the efficacy of newly developed capture processes because of their high reliability in industries.

Three methods for improving the efficiency of the chemical absorption process and reducing its total operating cost and energy consumption for solvent regeneration have shown continuous improvements. First, many studies have reported the development of new solvents or blends as an attractive approach. Second, changes in operating conditions and equipment design have been suggested as a possible means of improving efficiency. The influence of operating conditions, such as liquid to gas ratio and reboiler energy, on performance has been studied using dynamic simulations [5, 16, 17]. Furthermore, the performance of a process at a steady state has also been evaluated as the device design and operating conditions were changed [6, 18]. Finally, a new process configuration has been introduced to reduce capital expenditure (CAPEX) and operational expenditure (OPEX). Based on the utilization of the same absorbent, new process configurations have reported the potential to reduce energy consumption in solvent regeneration via heat integration and different stream methods [19-21]. As shown in Table 1, many studies on the modification of a stripper have conducted performance evaluations for various single and combined modified configurations at specific conditions. Each study suggested the energy efficiency and advantage of a specific

configuration. However, because the studied reference conditions, such as reference operating data, CO_2 concentration, flow rate, and/or temperature of flue gas, are clearly different, a direct comparison of the advantages among configurations is not reasonable even if the same configuration is applied for different reference conditions.

Table 1. Literature review of process modifications of the strippers in CO_2 capture with amines [17, 18, 22-31].

Recent work within the industry has also demonstrated interest in the development of process configurations that can achieve a higher efficiency. This has led to the application of new process configurations and operations in power plants [32, 33]. Because the capture performance highly depends on the operating conditions of the modified configuration, not all modified configurations will always improve efficiency. Therefore, a sensitivity analysis of the variation of operating conditions was needed for modified configurations. In addition, because the modification of a conventional configuration inevitably increases a capital cost by equipping additional devices and utilities such as compressors, heat exchangers, and flash drums, etc., the simultaneous progress in economic analysis is also essential. Furthermore, to elucidate the energy efficiency and cost by process modification, modified configurations must be evaluated at the same reference condition. And the savings-to-investment ratio (SIR) can be an indicator between the added device cost and the reduced operating cost in the configurations for carbon capture.

In this study, a techno-economic analysis of new process configurations for heat integration was conducted to reduce the operating cost and energy consumption in solvent regeneration. For energy reduction during regeneration of CO_2-rich MEA solvent, various modified configurations were applied to a stripper: lean vapor compression (LVC), cold solvent split (CSS), and stripper overhead compression (SOC). The LVC that has been applied to many processes has been widely researched, and the SOC can serve as a heat pump and reduce energy consumption for CO_2 compression and storage. The CSS was reported to improve efficiency through modifying stream configurations as shown in Table 1. The configurations combined with two or more of components were designed at the same reference condition. The performances of eight configurations (three single modifications and five combined configurations) were analyzed and compared with the reference data from a CASTOR/CESAR pilot plant [34, 35]. A sensitivity analysis of the combined configurations

was also conducted according to the change of operating conditions. An economic analysis was conducted on all the process configurations using a 300-MW full-scale power plant. With respect to savings-to-investment ratio (SIR), the optimum configuration and advantages of configuration were also discussed under the same reference condition because additional devices and utilities for modification can increase costs and reduce energy consumption. We deem that the proposed configurations can provide comparative information among various feasible configurations when installing new CO_2 capture plants or retrofitting existing CO_2 capture plants.

2. Process description

2.1 The conventional MEA process as a reference process

The operational results from a CASTOR/CESAR pilot plant were selected for validating the simulation and to act as a comparative reference. The selected pilot plant used MEA and captured CO_2 from flue gas released from a 10-MW pulverized bituminous coal power plant [34, 35]. This conventional MEA process consisted of an absorber, stripper, and rich-lean solvent heat exchanger as shown in Fig. 1. The process can capture 90% of the incoming carbon in flue gas flowing at a rate of 5000 Nm^3/h. The operating conditions for the MEA process are listed in Table 2.

Fig. 1. A process flow diagram for the referenced MEA process [34, 35]

Table 2. Operating conditions of the referenced process [35, 36] and the modified processes

The stripper in the referenced process consisted of a 17.0 m packing section and 3.0 m water wash section. The inner diameter of the stripper was 1.1 m. The packing section began from the bottom of the tower, and the water washing section was located at the top to reduce MEA losses. The water washing section was packed with Sulzer Mellapak 2X. The flue gas (11% CO_2), which was passed through the wet flue gas desulfurization (FGD), entered from the bottom of the tower. As shown in Fig. 1, the rich-solvent from the bottom of the stripper was heated to 105 ℃ by a heat exchange process, with the lean-solvent being recovered from the stripper. The rich-solvent was then supplied to the middle of the stripper to a packing height of 10.0 m (inner diameter of a 1.1-m) and additional water washing section of

3.0 meter (reduced inner diameter of a 0.8-m) from the top of the stripper. Both the sections were further filled with Sulzer Mellapak 2X [35, 36].

The regenerated amine solution (30 wt.% MEA) was cooled to 40 ℃ by a heat exchanger containing the rich-solvent. It was then fed between the packing section and water washing section of the stripper. The separated CO_2 was released from the top of the stripper. For transportation, the water vapor in the produced CO_2 was removed to <500 ppm and to avoid pipeline corrosion [37]. Afterwards, the dried CO_2 was compressed to 152.7 bar using a multi-stage compressor for transportation and storage [31, 38].

2.2 Modified configurations of the stripper

Several modified configurations have been reviewed in previous studies [19, 20]. The main concern for developed configurations to improve the efficiency was to modify heat integration in a stripper unit. The schematic diagram for each modified configuration is shown in Fig. 2; these configurations include lean vapor compression (LVC), cold solvent split (CSS), and stripper overhead compression (SOC) [22, 31, 39].

Fig. 2. A process flow diagram for alternative MEA processes [33-35]: (a) LVC, (b) CSS, (c) SOC case 1, and (d) SOC case 2

The principle of the LVC configuration is as follows: the lean-solvent at the bottom of the stripper is flashed. As the temperature of the lean-solvent decreases during this step, it is separated at the vapor-liquid equilibrium (VLE) state into liquid and vapor phases in a flash drum. The composition of the vapor primarily consists of H_2O and CO_2. The separated vapor is compressed and supplied to the bottom of the stripper, and the separated lean-solvent is then transported to the rich-lean solvent heat exchanger by a pump.

As CO_2 is further separated by the decompression of the lean-solvent, reboiler energy can be saved. Additional heat can be supplied to the amine solvent in the stripper because the compressed vapor from the flash drum is fed to the bottom of the stripper at a high-temperature. This contributes to reducing the reboiler energy. On the other hand, additional energy of compression for the vapor is required in the process configuration, as shown in Fig. 2(a). Furthermore, because of the lean solvent's decreased temperature following decompression, it can transfer only a small amount of thermal energy to the rich-solvent in the rich-lean-solvent heat exchanger. In this study, it was assumed that the lean-solvent was

flashed to 1.05 bar. The vapor was to be transported to the bottom of the stripper and was compressed to 2 bar by a compressor.

In the CSS configuration (Fig. 2(b)), the main characteristic of the process is the split flows of the rich-solvent at different temperatures. A part of the rich-solvent from the absorber is directly supplied to a stripper; therefore, its flow into the heat exchanger is relatively lesser than in the other configurations without the split flow. The remaining part of the rich-solvent that is sent to the heat exchanger can be heated more than in the other configurations. As the high-temperature rich-solvent is supplied to the stripper, energy consumption by the reboiler can be saved. Furthermore, the low-temperature rich-solvent that does not pass through the heat exchanger enters the top of the stripper and contacts the high-temperature CO_2 gas rising to the top of the stripper. Because the low-temperature rich-solvent can recover heat from CO_2 gas, the energy consumption by the condenser and reboiler can be reduced. However, the heat transfer efficiency of the lean-rich-solvent heat exchanger can decrease because the vapor may be generated from the rich-solvent heated to a higher temperature. When considering the CSS configuration, it is necessary to determine the split ratio of the rich-solvent sent to the top of a stripper and to the heat exchanger. In this study, the split ratio was optimized to minimize overall energy consumption for CO_2 capture.

The main feature of the SOC configuration is the compression of the effluent vapor coming from the top of the stripper before it enters the condenser. As the temperature of the compressed vapor is increased, it can be used to provide heat to other streams. In this study, the compressed vapor stream was used as an energy carrier to increase the solvent temperature before it entered the reboiler as shown in Fig. 2(c) (SOC case 1), or before it entered the stripper as shown in Fig. 2(d) (SOC case 2).

The captured CO_2 was compressed to 152.7 bar for transportation and storage. The CO_2 compression process consists of a 5-stage compressor: 4.56, 11.6, 29.5, 75, and 152.7 bar [39, 40]. A part of the compressor unit can be utilized for SOC configuration. A comparative analysis was conducted when the vapor was compressed to the range of 3 to 11.6 bar. It was considered that the vapor could be compressed to below 4.56 bar by a single-stage compressor, while a two-stage compressor could compress the vapor from 4.56 to 11.6 bar. Furthermore, a cooler was installed between each stage to prevent the temperature of the gas from increasing because of compression. In this study, the heat that resulted from the compression was supplied to the reboiler as shown in Fig. 2(c).

After evaluating the efficiency of each individual configuration, the combined process configurations were developed to confirm their feasibility for a further improvement in stripper efficiency. Four different configuration combinations were designed as shown in Figs. 3 and 4: LVC with CSS, SOC with LVC, SOC with CSS, and SOC with LVC and CSS.

Fig. 3. Process flow diagrams for (a) LVC combined with CSS, (b) SOC combined with LVC, and (c) SOC combined with CSS

Fig. 4. A process flow diagram for SOC combined with LVC and CSS

In the configuration of LVC with CSS (Fig. 3(a)), the compressed vapor from the flash drum is fed to the bottom of the stripper at a high-temperature. Moreover, in the CSS configuration, the low-temperature rich-solvent contacts the high-temperature CO_2 gas rising to the top of the stripper and recovers heat from the CO_2 gas at the top of the stripper. Therefore, the advantage noted in this study was that LVC and CSS individually contributed to the stripper. However, only a small amount of thermal energy could be transferred to the rich-solvent in the rich/lean-solvent heat exchanger; this is a disadvantage of LVC because even CSS cannot recover this energy.

In the configuration of SOC with LVC (Fig. 3(b)), the SOC case 2 configuration can offset the disadvantage of the LVC configuration mentioned previously. On the other hand, because the SOC case 1 configuration works only as a heat pump, there is no interaction with the LVC configuration. It is the same as the configuration of SOC case 1 with CSS in Fig. 3(c). In SOC with CSS, unlike SOC with LVC, the temperature of the rich-solvent from the rich/lean-solvent heat exchanger is higher than that of the reference configuration because of the CSS configuration. On the other hand, if a certain degree of heat is supplied to the SOC case 2 configuration, operational risk may increase because of increased vapor generation in the heat exchanger.

In the configuration of SOC with LVC and CSS (Fig. 4), because the LVC configuration decreases the temperature of the rich-solvent from the rich/lean-solvent heat exchanger, the risk posed by the vapor generated inside the heat exchanger, which resulted from the additional heat supply in the SOC case 2 configuration, can be reduced. The shortcomings of each single modification are expected to be compensated through the benefits of LVC with CSS as well as the previously mentioned heat pump effect in SOC case 1.

3. Simulation methodology

The process simulation of the amine-based absorption/desorption processes was performed with Aspen Plus v.8.8 (Aspen Technology Inc., USA). The simulation validation of the referenced amine process (Fig. 1) has been reported in previous studies [35, 41]. Information about and the specifications of the main units are presented in Table 3 [35, 36, 42, 43]. The absorber and the stripper were simulated using a rate-based calculation model. In this model, the heat of the reaction between MEA and CO_2, the heat of water evaporation, and the heat exchange between the liquid and vapor phase were reflected in the liquid phase, while the heat exchange between liquid and vapor was reflected in the vapor phase. The absorption amount of CO_2 was also evaluated using a mass transfer rate between liquid and vapor phases rather than reaching equilibrium. All process configurations were studied to minimize energy consumption under the same solvent loading flow rate, where the carbon removal efficiency was greater than 90%. In the simulation, the temperature of the reboiler was adjusted to achieve a CO_2 removal efficiency of higher than 90%. Therefore, the temperature was slightly different among the configurations, but it was determined at approximately 120 ^{o}C. Because the fluid was in the VLE state in the reboiler, the change in fluid temperature was small even if the thermal energy was supplied more or less.

Table 3. Specifications of the main units [35, 36, 42, 43]

3.1 Thermodynamics and kinetics

All the devices were modeled using the electrolyte nonrandom two-liquid (e-NRTL) activity coefficient model and the Redlich-Kwong (RK) equation of state for the liquid and gas phases, respectively [44]. The kinetic model, expressing the reaction rate between CO_2 and aqueous amine, has a significant impact on the simulation results. In this study, the Aspen plus kinetic model, as based on the Hikita kinetics model, was used [35, 45-47]. The reactions of CO_2 with the aqueous MEA are as follows:

$$2H_2O \leftrightarrow H_3O^+ + OH^- \quad (1)$$

$$MEA^+ + H_2O \leftrightarrow MEA + H3O^+ \quad (2)$$

$$HCO^{3-} + H_2O \leftrightarrow CO_3^{2-} + H_3O^+ \quad (3)$$

$$HCO^{3-} \leftrightarrow CO_2 + OH^- \quad (4)$$

$$MEA + H_2O + CO_2 \leftrightarrow MEACOO^- + H_3O^+ \quad (5)$$

3.2 Economic analysis

A cost evaluation is essential for any feasibility study. In this study, important economic indicators, including capital and operating costs, were evaluated. The volume capacity increased by a factor of 3, while the surface constituting the device was multiplied by a factor of 2 [48]. Thus, the material cost per unit volume and the capital cost per unit net power production were lowered with an increase in the system capacity. Because the capital cost per unit net power production can be unreasonably high for pilot scale power plants, as presented in Table 2 (flue gas of 4974.92 Nm^3/h), the cost evaluation for the equipment and material was conducted for a 300-MW full scale coal power plant [49, 50]. In this study, an economic analysis was conducted assuming the flue gas flow of a 300-MW full scale plant working at a rate of 1,200,000 Nm^3/h (11 mol.% CO_2).

The capital cost included the equipment, material, and other direct and indirect costs. The operating cost included variable operating costs and the fuel cost but did not include fixed operating costs. This is because the fixed operating costs depend strongly on the policies and economic situation of each country. The equipment and material costs were calculated using the performance analysis results and the Aspen Economic Analyzer v.8.8 [51]. It was assumed that the sum of the equipment costs and material costs accounted for 30% of the capital cost [52]. Utility consumption, including cooling energy, steam, and electricity, was calculated from the process simulation results. In this study, the cooling water was assumed to be supplied at 20 ^oC and used at up to 25 ^oC. The cooling water flow rate was determined by the required cooling duty in process simulation. The low-pressure steam at 125 ^oC was used for reboiler heating until it reached 124 ^oC. As with the cooling water, the flow rate of the low-pressure steam was determined depending on the heat duty required by the reboiler. The prices of steam, electricity, and cooling energy were assumed to be 5.1×10^{-6} US$/kJ, 0.0775 US$/kWh, and 2.12×10^{-7} US$/kJ, respectively, based on the Aspen Economic Analyzer v.8.8.

4. Simulation results and discussion

The amine-based absorption/desorption process requires two types of energy: electrical energy used by the compressor and the pump, and thermal energy for the reboiler. To compare the energy efficiency among different process configurations, it was necessary to

combine the two types of energy into one using equivalent work. The energy obtained from converting thermal energy into electrical energy was considered as the equivalent work done by thermal energy. Therefore, the total equivalent work (W_{total}) of the process was the summation of the equivalent work done by both thermal and electrical energies.

The W_{total} for each process configuration was calculated by the following equation [19]:

$$W_{total} = \eta_{turbine} \times \frac{T_{source} - T_{sink}}{T_{source}} \times Q_{thermal} + W_{electrical} \qquad (6)$$

Where $\eta_{turbine}$ is the turbine efficiency, 0.75, T_{source} is the source temperature (438 K), T_{sink} is the sink temperature (300 K), $Q_{thermal}$ is the thermal energy, and $W_{electrical}$ is the electrical energy [31].

The results from the CESAR CO_2 pilot plant Test 1A-2, which is the reference of this study, were used to verify the accuracy of the simulation results. In Fig. 5, the evaluated temperature profiles in the absorber and stripper columns were compared with the reference operating data [41]. The simulation temperature was on average 2.6 % higher than the experimental value. This is because the simulation using the rate-based model in Aspen Plus does not reflect the heat loss from the absorber column to the ambient air. On the other hand, the simulation temperature in the stripper was on average 1.53 % lower than the experimental temperature, which mainly resulted from the lower temperature of the rich-solvent at the top of the stripper (2.6% difference). When considering the accuracy and sensitivity of temperature sensors, the inside temperatures of the absorber and stripper columns were reasonably predicted in the simulation. The reboiler duty from the reference operating result was measured as 3.6 GJ/tonCO_2, and the simulation result was 3.72 GJ/tonCO_2.

Fig. 5. Temperature profiles of experimental data [41] and simulation results for the reference process: (a) absorber and (b) stripper.

4.1 Effect of a single modification on the process

The main effects of LVC in Fig. 2(a) were to heat the bottom of the stripper and to flash the lean-solvent. As shown in Fig. 6, the temperature at the bottom of the stripper was higher than that of the reference process shown in Fig. 1 because the high-temperature lean vapor entered the bottom of the stripper. After a steep decrease in temperature along the tower, the temperature at the middle and the top of the stripper became almost constant. The temperature was lower than that of the reference configuration because the temperature of the

rich-solvent entering the middle height of the stripper was lower, as shown in Fig. 2(a). As a result, more CO_2 was desorbed from the rich-solvent at the bottom of the stripper (Fig. 7). After a steep increase in the CO_2 flow rate till a height of 2–3 m in the tower, the CO_2 flow rate became almost constant along the tower. At position A specified in Figs. 6 and 7, where the rich-solvent was fed, the temperature and desorbed CO_2 flow rate were slightly decreased. Because the vapor temperature at the top of the stripper was lower than that of the reference configuration, water content in the overhead vapor was also lower, leading to lower cooling energy requirements of the condenser. As a result, as indicated in Table 4, a 90% carbon capture could be achieved with a W_{total} that was 4.83% lower than the work required in the reference configuration.

Fig. 6. Temperature profiles of the vapor phase in a stripper for all the cases under the optimum operating condition: "A" indicates the position of rich-solvent supply

Fig. 7. Flow rate profiles of CO_2 in vapor phase in a stripper for all the cases under the optimum operating condition: "A" indicates the position of rich-solvent supply

Table 4. Performance assessment of reference and modified strippers under the optimum operating condition

The main feature of CSS (Fig. 2(b)) is to cool the top of the stripper by splitting the flow of the rich-solvent. Because the low-temperature rich-solvent sent to the top of the stripper absorbs heat and desorbs CO_2, the reboiler duty can be reduced. After maintaining a similar temperature at the bottom of the stripper, the temperature along the tower became higher than that of the reference configuration, as shown in Fig. 6. However, because of the split stream of the low-temperature rich-solvent, the temperature at the top of the stripper became lower as well, which led to absorption of heat in the stripper. As shown in Fig. 7, after position A in the stripper, the CO_2 flow rate continually increased until the gas reached the top, leading to a differently shaped flow rate profile as compared to other single modified process configurations. This indicated that the reboiler and condenser cooling energies were reduced by the absorption of heat and by maintaining a lower temperature at the top of the stripper, respectively.

The equivalent work in the CSS-related configurations were considerably affected by the split ratio of the rich-solvent sent to the top of the stripper and the heat exchanger. Figure 8 shows the equivalent woks at various split ratios for the CSS-related configurations. When

the split ratio was excessively high, the equivalent work increased from the minimum because the amount of cold rich-solvent sent to the top of the stripper was excessively small, and the thermal energy at the top of the stripper could not be recovered sufficiently. If the split ratio was excessively small, the amount of rich-solvent sent to the rich/lean-solvent heat exchanger became excessively small, and the temperature of the rich-solvent inside the rich/lean-solvent heat exchanger increased excessively. As a result, the lean-solvent could not transfer sufficient thermal energy. The CSS-related configurations were evaluated at a fixed split ratio to achieve the minimization of equivalent work. With the CSS modification, an 8.11% reduction in reboiler energy and a 5.76% reduction in the W_{total} was achieved in the optimum operating condition presented in Table 4.

Fig. 8. Variation of equivalent work as a function of the split ratio: (a) CSS and CSS with SOC (b) LVC with CCS and SOC with LVC and CSS.

In the case of SOC modification, the variation in W_{total} depended on the supplementation of heat from the compressed vapor at high temperatures. For SOC case 1, the generated heat was transferred to the lean-solvent before it entered the reboiler, as shown in Fig. 2(c). Therefore, because SOC case 1 did not affect the stripper inlet stream, the temperature profile and CO_2 flow rate were the same as those in the reference configuration, as depicted in Figs. 6 and 7.

As mentioned previously, the SOC configuration was evaluated when the vapor was compressed in the range of 3 to 11.6 bar. As the dew point of the compressed vapor increased with pressure, the latent heat of the vapor could be transferred to the amine solvent. Therefore, the more the stripper overhead vapor was compressed, the less W_{total} was required, as shown in Fig. 9. W_{total} steeply decreased until 7.5 bar, but it increased smoothly with further compression in the SOC case 1 configuration. However, at lower than 3.8 bar, W_{total} was higher than that in the reference configuration because the electrical energy consumption by the overhead vapor compression was greater than the thermal energy transferred to the lean-solvent.

A 2-stage compressor was required to increase the vapor pressure to higher than 4.56 bar. As only gas phase components without any liquid should enter each stage of the compressor, the vapor from the first stage compressor could transfer heat before it reached the dew point temperature. When the stripper overhead vapor was compressed to a pressure higher than 7.5

bar, the available thermal energy in the first stage decreased because of an increase in the dew point temperature. Therefore, W_{total} began to increase smoothly with pressure. With the SOC case 1 modification, a 5.08% reduction in W_{total} as compared to the reference configuration could be achieved in the optimum condition with a 27.9% reduction in reboiler energy. However, W_{total} was almost equivalent to that of LVC or less than that of the CSS (Fig 7).

Another configuration of SOC was also possible, where the heat was transferred to the rich-solvent before it entered the stripper as shown in Fig. 2(d) (SOC case 2). The highest temperature profile was maintained along the stripper (Fig. 6). Therefore, although the CO_2 flow rate was relatively lower than in other process configurations, it steeply increased at position A shown in Fig. 7, where the rich-solvent was fed. Furthermore, it led to an increase in the amount of water content in the vapor at the top of the stripper. This has been discussed later in this report (Fig. 10).

The compressed stripper overhead vapor met a stream at a lower temperature as compared to SOC case 1. Thus, when the stripper overhead vapor was compressed to below 3.7 bar, SOC case 2 could transfer more heat to the cold stream. In this case, W_{total} became lower than that in the reference configuration and SOC case 1. However, as the overhead vapor was compressed further, there was a significant increase in W_{total}, as shown in Fig. 9. The higher the amount of water in the overhead vapor, the more electrical energy was required for compression. Therefore, with the configuration of SOC case 2, a 0.6% reduction in W_{total} could be achieved under optimum conditions, even showing a 15.5% reduction in reboiler energy as presented in Table 4.

Fig. 9. Effect of compressed outlet pressure of the overhead vapor in a stripper on total equivalent work (Reference resulted from Tables 1 and 2, and Fig. 5)

4.2 Performance assessment of combined configurations

Considering the characteristics of every individual configuration, the process modification of the stripper by different combinations of individual configurations were designed and evaluated. When the LVC was combined with CSS, as shown in Fig. 3(a), a 7.81% reduction in W_{total} was achieved in the optimum conditions presented in Fig. 9 and Table 4; additionally, a 21.8% reduction in reboiler energy was achieved.

The advantages of the LVC configuration were compensated by the CSS configuration, i.e., the amount of rich-solvent sent to the rich-lean-solvent heat exchanger was reduced, and the

temperature of the rich-solvent entering the stripper was increased, as shown in Fig. 6. As a result, some of the CO_2 in the rich-lean solvent heat exchanger was desorbed, which could reduce the duty of the reboiler. Furthermore, at the top of the stripper, CO_2 was desorbed by the contribution of the CSS configuration; thus, the reboiler energy was further reduced.

As shown in Figure 6, in the LVC-related configurations, the temperature at the middle of the stripper was lower than the reference case. Therefore, even if the cold rich-solvent was added to the top of the stripper, the amount of thermal energy, which could be recovered in the top of the stripper, was smaller than the other configurations. As a result, when the LVC modification was included in the configurations, thermal energy could be recovered sufficiently at the top of the stripper even if the amount of the cold rich-solvent sent to the top of the stripper was reduced. Therefore, as shown in Figures 8 (a) and (b), the configuration of CSS with LVC consumed less energy when the split ratio was higher than only the CSS modification.

When the LVC configuration was combined with the SOC configuration, there was further reduction in W_{total} (Fig. 9). When the overhead vapor was compressed below 4.56 bar, heat was transferred through stream 1, as shown in Fig. 3(b), because the temperature of the cold incoming stream 1 was lower than that of stream 2, as mentioned in the SOC case 2 configuration. However, when being compressed over 4.56 bar by a 2-stage compressor, if all the heat was transferred to stream 1, an increase in W_{total} is observed because of the same reason as that observed for SOC case 2.

As an alternative, vapors from first and second compressors could transfer the heat through stream 2 and stream 1, respectively, as shown in Fig. 3. In this case, heat transfer via the vapor from the first compressor was limited to the cold incoming flow only until the vapor reached the dew point.

On the other hand, the vapor from the second compressor could transfer heat until the temperature reached a minimum approach temperature. Therefore, it transferred more heat when it contacted a cold incoming stream at a lower temperature in a heat exchanger. The temperature of cold incoming stream in stream 1 was lower than that in stream 2. As shown in Fig. 9, W_{total} decreased with pressure till 5 bar. However, if the overhead vapor was compressed over 5 bar, W_{total} gradually increased because of the same reason as in SOC case 1 and SOC case 2. The configuration based on combination of LVC with SOC provided a 7.41% reduction in W_{total} in the optimum condition with a 32.8% reduction in reboiler energy.

When the SOC configuration was combined with the CSS configuration in Fig. 3(c), no significant changes were observed in the performance, as shown in Fig. 9. The temperature of the vapor after compression was also relatively low as compared to other configurations. Additionally, the temperature did not become high even when the stripper overhead vapor was compressed further. Therefore, the performance was not improved because the transfer of thermal energy was limited to the cold incoming stream at a relatively high temperature. As a result, the temperature and CO_2 flow rate profiles in the stripper were similar to those in the CSS configuration, as depicted in Figs. 6 and 7 before the position A. Above position A, the temperature of the stripper reduced because of an increased rich-solvent flow into the top of the stripper. The rich-solvent absorbed slightly more heat at the top of the stripper. As a result, the reboiler energy was reduced by 10.9%, but there was a 5.77% reduction in W_{total} that was similar to only the CSS configuration.

A last configuration was developed by combining all three single configurations (LVC, CSS, and SOC) as shown in Fig. 4. The heat generated by overhead vapor compression was transferred in the same way as in the configuration combining LVC and SOC. The vapor temperature was relatively low because of the CSS configuration, even though it was higher than that in the LVC configuration and the configuration combining LVC and SOC. Therefore, the water content in the overhead vapor was also low. This led to a lower electrical energy consumption in the overhead vapor compressor. However, it also led to a lesser reduction in reboiler energy in the SOC configuration.

On the other hand, if the temperature of the vapor coming from the top of the stripper was excessively low, the effect of SOC on the combined configuration was excessively reduced. Thus, as presented in Table 4, the split ratio of the proportions of rich-solvent that flowed to the top of the stripper and to the heat exchanger was less than those in the other CSS configurations (CSS, LVC+CSS, and CSS+SOC) in the optimum operating condition. When the ratio in the splitter was adjusted appropriately, both the reboiler energy and the electrical energy consumption in the overhead vapor compressor was reduced as compared to in the other configurations, except for the SOC+LVC configuration.

In summary, as compared to the configuration combining SOC and LVC, the reboiler energy was increased by 1.69%, but the electrical energy was reduced by 5.73%. As a result, SOC with LVC and CSS showed the lowest energy consumption and 9.01% reduction in W_{total}, along with a 31.6% reduction in reboiler energy within the optimum conditions presented in Table 4. However, since the addition of devices and utilities for the modification

leads to an increase of capital cost, it should be evaluated whether it is worth not only from an energy saving point of view, but also from an economic point of view. This will be discussed in the next section.

Figure 8 shows a comparative summary of the performances of all the configurations. Owing to the characteristics of each configuration, the energy consumptions by the reboiler and compressor were different, but the energy performance had to be evaluated with respect to overall energy consumption. Furthermore, the overhead water vapor flow rate was one of the key factors that helped decide the configuration with respect to environmental issues, as well as reliable operation. In this study, from the viewpoint of energy consumption and water vapor content, the configuration that combined SOC, LVC, and CSS was the most efficient, but the complexity in the configuration should be evaluated in more detail in further engineering studies after energy-based and economic evaluations.

Fig. 10. Overhead water vapor flow rate and vapor compression energy/reboiler duty in a stripper at the optimum operating condition

4.3 Economic evaluation

The cost evaluation for all the configurations is listed in Table 5. In the case of LVC-applied configurations, a flash vessel to separate the vapor from the flashed lean-solvent and a compressor to compress the lean vapor were additionally required. Therefore, the cost of the compressor increased according to the required compression pressure. In the case of CSS-applied configurations, only an additional part was responsible for splitting the flow of the cold rich-solvent. On the other hand, the cost of the rich-lean solvent heat exchanger was reduced because the rich-solvent flow toward the heat exchanger was reduced. In the case of SOC-applied configurations, an additional heat exchanger was required to transfer the additional heat generated by the compressor. The compressor for the overhead vapor from the top of the stripper was not counted in the capital cost because it was considered as a part of the CO_2 compressor for transportation and storage after CO_2 capture. However, because the overhead vapor contained a relatively large amount of water content at a higher temperature, the volumetric flow rate was higher than that in the reference configuration. Thus, the total compressor cost was higher than that for the reference configuration because of the presence of a compressor with a larger capacity. The capital cost was generally high when the LVC-based configuration was used. It resulted from a large volume flow rate of lean vapor at low

pressure (about 1.05 bar). Therefore, the cost of the lean vapor compressor led to an increase in the capital cost.

As presented in Table 5, adding an auxiliary configuration to the reference configuration did not always increase the capital cost of the entire process because the components in the processes were different among the process configurations. The increase in capital cost by an addition of the LVC configuration was higher than that by the addition of the SOC configuration. With respect to energy saving, combined configurations showed a better performance than the single modification. The results mainly focused on savings in steam energy, but a certain level of offset occurred that was mainly caused by increased electrical energy consumption.

Table 5. Comparison of capital and operating costs among the modified carbon capture processes based on a 300-MW power plant

Table 6 presents the capital and operating costs that could be saved by each configuration as compared to the reference configuration. The savings-to-investment ratio (SIR) was calculated by dividing the operating cost savings during the project lifetime by the capital cost change. A ratio of greater than 1.0 indicated an economically feasible project [53].

The CSS configuration and the combined configuration of SOC and CSS had lower capital and operating costs than the referenced configuration. Thus, these configurations were satisfactory alternatives for the referenced MEA process because they reduced all relevant expenses. Upon their exclusion, SOC case 1 had the highest SIR. Although the increase in capital cost was somewhat high, the SOC with LVC and CSS may also be considered a potential candidate for the MEA process, as energy efficiency was the most important factor.

Figure 11 shows the sensitivity analysis results for SIR as a function of utility cost. The variation of SIR was evaluated when the unit price of steam and electricity was changed by ±10%. In the reference configuration, the operating cost mainly resulted from steam usage in the reboiler. Therefore, the SIR values of all the configurations increased with the unit price of steam. In contrast, the SIR values were reduced with an increase in electricity price because the electricity was mainly used by a compressor. In the SOC case 1 configuration, the SIR value was highly affected by the utility unit price because the utility usage composition of SOC case 1 configuration was different compared to the reference configuration. The SOC modification resulted in greatly reducing the steam consumption

because of the reduction of the reboiler duty, but the electricity consumption in the compressor could be highly increased. In addition, SOC case 2 seemed to be a non-feasible modification with respect to the SIR result, regardless of energy savings. Moreover, the SIR value might become lower than 1 in the cases of LVC and LVC with SOC if the utility unit price is significantly changed.

Table 6. Comparison of cost savings based on assessment of a 300-MW power plant

Fig. 11. Sensitivity analysis results for savings-to-investment ratio as a function of utility cost: (a) steam cost and (b) electricity cost

5. Conclusions

A techno-economic analysis of various configurations of heat integration was conducted for efficient post-combustion carbon capture. All modified process configurations aimed to reduce the energy consumption of solvent regeneration in the stripper and the operating cost. In all configurations, flue gas with the same temperature, pressure, composition, and flow rate entered the stripper, and the same flow rate of 30 wt.% MEA solvent was allowed. When a 90% carbon capture was achieved, the energy consumption of each configuration was compared and analyzed.

The energy consumption was investigated by the equivalent work, which was a combination of thermal energy consumed during solvent regeneration and electrical energy used by the compressor and pump. All the modifications were optimized to minimize the total equivalent work. The economic analysis was conducted assuming a 300-MW full-scale power plant. The operating and capital costs were based on equipment cost and were calculated for each configuration.

All the configurations achieved a reduction in the reboiler energy in the range of 8.11% to 32.8% at optimum operating conditions. In the case of the configuration with SOC and LVC, the highest reduction in the reboiler energy of 32.8% was achieved. A 0.6% to 9.0% reduction in W_{total} was also accomplished using these configurations in optimum operating conditions. Primarily, by using a new configuration of the stripper, SOC with LVC, and CSS, a W_{total} of 49.59 kJ/mol CO_2 was achieved, which was a significant reduction of 9.0% from the conventional configuration.

The economic evaluation indicated that all configurations were economically feasible where the project lifetime was considered as 20 years, except for the SOC case 2 configuration. Specifically, in the CSS configuration and the combination of SOC with CSS, both the capital and operating costs were reduced as compared to those for reference configuration. However, in the configurations with LVC, a large increase in capital cost occurred owing to the high cost of the lean vapor compressor in the LVC modification. Considering only the operating cost, the configuration combined with SOC, LVC, and CSS was recommended because it had the highest energy savings. However, because of this configuration's complexity, operational difficulty should be reviewed in further studies. According to the SIR evaluation, the SIR values in all the configurations were significantly affected by the change in utility unit cost. The SIR values of the SOC case 1 and LVC with CSS were higher than the combined configuration of SOC with LVC and CSS, regardless of the change of utility cost. However, because of the high dependence on capital costs in each country, a more detailed investigation is needed in engineering designs.

Acknowledgments

This work was supported by Korea Institute of Energy Technology Evaluation and Planning (KETEP) grant funded by the Korea government (MOTIE) (20172010202070, Development of upgrading technology for the post-combustion advanced amine CO_2 capture related to Mid-scale CO_2 storage)

Reference

[1] International Energy Agency, World Energy Outlook. https://webstore.iea.org/world-energy-outlook-2018/, 2018.

[2] National Energy Technology Laboratory, Carbon capture program. https://www.netl.doe.gov/sites/default/files/2017-11/Program-115.pdf/, 2017.

[3] Y.S. Ju, C.H. Lee. Dynamic modeling of a dual fluidized-bed system with the circulation of dry sorbent for CO_2 capture, Appl. Energy 241 (2019) 640-51.

[4] Y.S. Ju, H.T. Oh, C.H. Lee. Sensitivity analysis of CO_2 capture process in cyclic fluidized-bed with regeneration of solid sorbent, Chem. Eng. J. (2019) 122291.

[5] M.S. Walters, T.F. Edgar, G.T. Rochelle. Dynamic modeling and control of an intercooled absorber for post-combustion CO_2 capture, Chem. Eng. Process. 107 (2016) 1-10.

[6] H. Jilvero, F. Normann, K. Andersson, F. Johnsson. The Rate of CO_2 Absorption in Ammonia Implications on Absorber Design, Ind. Eng. Chem. Res. 53 (2014) 6750-8.

[7] W.S. Lee, H.T. Oh, J.C. Lee, M. Oh, C.H. Lee. Performance analysis and carbon reduction assessment of an integrated syngas purification process for the co-production of hydrogen and power in an integrated gasification combined cycle plant, Energy 171 (2019) 910-27.

[8] J.P. Ciferno, T.E. Fout, A.P. Jones, J.T. Murphy. Capturing carbon from existing coal-fired power plants, Chem. Eng. Prog. 105 (2009) 33-41.

[9] Z.H. Liang, T. Sanpasertparnich, P.P.T. Tontiwachwuthikul, D. Gelowitz, R. Idem. Part 1: Design, modeling and simulation of post-combustion CO_2 capture systems using reactive solvents, Carbon Manage. 2 (2011) 265-88.

[10] M. Bui, I. Gunawan, V. Verheyen, P. Feron, E. Meuleman, S. Adeloju. Dynamic modelling and optimisation of flexible operation in post-combustion CO_2 capture plants—A review, Comput. Chem. Eng. 61 (2014) 245-65.

[11] X. Chen, F. Closmann, G.T. Rochelle. Accurate screening of amines by the Wetted Wall Column, Energy Procedia 4 (2011) 101-8.

[12] M. Afkhamipour, M. Mofarahi. Review on the mass transfer performance of CO_2 absorption by amine-based solvents in low-and high-pressure absorption packed columns. RSC advances 7 (2017) 17857-72.

[13] S.Y. Choi, S.C. Nam, Y.I. Yoon, K.T. Park, S.J. Park. Carbon dioxide absorption into aqueous blends of methyldiethanolamine (MDEA) and alkyl amines containing multiple amino groups. Ind. Eng. Chem. Res. 53 (2014) 14451-61.

[14] I. Sreedhar, T. Nahar, A. Venugopal, B. Srinivas. Carbon capture by absorption–path covered and ahead, Renewable Sustainable Energy Rev. 76 (2017) 1080-107.

[15] A. Wilk, L. Więcław-Solny, A. Tatarczuk, A. Krótki, T. Spietz, T. Chwoła. Solvent selection for CO_2 capture from gases with high carbon dioxide concentration, Korean J. Chem. Eng. 34 (2017) 2275-83.

[16] S.A. Jayarathna, B. Lie, M.C. Melaaen. Dynamic modelling of the absorber of a post-combustion CO_2 capture plant: Modelling and simulations, Comput. Chem. Eng. 53 (2013) 178-89.

[17] R. Dutta, L.O. Nord, O. Bolland. Prospects of using equilibrium-based column models in dynamic process simulation of post-combustion CO_2 capture for coal-fired power plant, Fuel 202 (2017) 85-97.

[18] K.Q. Jiang, K.K. Li, H. Yu, Z.L. Chen, L. Wardhaugh, P. Feron. Advancement of ammonia based post-combustion CO_2 capture using the advanced flash stripper process, Appl. Energy 202 (2017) 496-506.

[19] D.H. Van Wagener, G.T. Rochelle. Stripper configurations for CO_2 capture by aqueous monoethanolamine, Chem. Eng. Res. Des. 89 (2011) 1639-46.

[20] Y. Le Moullec, T. Neveux, A. Al Azki, A. Chikukwa, K.A. Hoff. Process modifications for solvent-based post-combustion CO_2 capture, Int. J. Greenhouse Gas Control 31 (2014) 96-112.

[21] F. Rezazadeh, W.F. Gale, G.T. Rochelle, D. Sachde. Effectiveness of absorber intercooling for CO_2 absorption from natural gas fired flue gases using monoethanolamine solvent, Int. J. Greenhouse Gas Control 58 (2017) 246-55.

[22] L. Dubois, D. Thomas. Comparison of various configurations of the absorption-regeneration process using different solvents for the post-combustion CO_2 capture applied to cement plant flue gases, Int. J. Greenhouse Gas Control 69 (2018) 20-35.

[23] K.Q. Jiang, K.K. Li, H. Yu, P.H.M. Feron. Piperazine-promoted aqueous-ammonia -based CO_2 capture: Process optimisation and modification, Chem. Eng. J. 347 (20 18) 334-42.

[24] S.Y. Oh, J.K. Kim. Operational optimization for part-load performance of amine-based post-combustion CO_2 capture processes, Energy 146 (2018) 57-66.

[25] S.Y. Oh, M. Binns, H. Cho, J.K. Kim. Energy minimization of MEA-based CO_2 capture process, Appl. Energy 169 (2016) 353-62.

[26] B. Zhao, F. Liu, Z Cui, C. Liu, H. Yue, S. Tang, Y. Liu, H. Lu, B. Liang. En

hancing the energetic efficiency of MDEA/PZ-based CO_2 capture technology for a 650 MW power plant: Process improvement, Appl. Energy 185 (2017) 362-75.

[27] K. Li, H. Yu, P. Feron, L. Wardhaugh, M. Tade. Techno-economic assessment o f stripping modifications in ammonia-based post-combustion capture process, Int. J . Greenhouse Gas Control 53 (2016) 319-27.

[28] K. Li, H. Yu, P. Feron, M. Tade, L. Wardhaugh. Technical and Energy Perform ance of an Advanced, Aqueous Ammonia-Based CO_2 Capture Technology for a 50 0 MW Coal-Fired Power Station, Environ. Sci. Technol. 49 (2015) 10243-52.

[29] K. Li, W. Leigh, P. Feron, H. Yu, M. Tade. Systematic study of aqueous mono ethanolamine (MEA)-based CO2 capture process: Techno-economic assessment of t he MEA process and its improvements, Appl. Energy 165 (2016) 648-59.

[30] Z. Liang, H. Gao, W. Rongwong, Y. Na. Comparative studies of stripper overhe ad vapor integration-based configurations for post-combustion CO_2 capture, Int. J. Greenhouse Gas Control 34 (2015) 75-84.

[31] J. Jung, Y.S. Jeong, U. Lee, Y. Lim, C. Han. New configuration of the CO_2 cap ture process using aqueous monoethanolamine for coal-fired power plants, Ind. En g. Chem. Res. 54 (2015) 3865-78.

[32] M. Bui, I. Gunawan, V. Verheyen, P. Feron, E. Meuleman. Flexible operation of CSIRO's post-combustion CO_2 capture pilot plant at the AGL Loy Yang power station, Int. J. Greenhouse Gas Control 48 (2016) 188-203.

[33] Y.J. Lin, E. Chen, G.T. Rochelle. Pilot plant test of the advanced flash stripper for CO_2 capture, Faraday Discuss. 192 (2016) 37-58.

[34] J.N. Knudsen, J.N. Jensen, P.J. Vilhelmsen, O. Biede. Experience with CO_2 capture from coal flue gas in pilot-scale: Testing of different amine solvents, Energy Procedia 1 (2009) 783-90.

[35] N. Razi, H.F. Svendsen, O. Bolland. Validation of mass transfer correlations for CO_2 absorption with MEA using pilot data, Int. J. Greenhouse Gas Control 19 (2013) 478-91.

[36] X. Luo, J. Knudsen, D. De Montigny, T. Sanpasertparnich, R. Idem, D. Gelowitz, et al. Comparison and validation of simulation codes against sixteen sets of data from four different pilot plants, Energy Procedia 1 (2009) 1249-56.

[37] National Energy Technology Laboratory, Quality Guideline for Energy System Studies: CO_2 Impurity Design Parameters. https://www.netl.doe.gov/energy-analysis/details?id= 789/, 2013.

[38] P.R. Jeon, D.W. Kim, C.H. Lee. Dissolution and reaction in a CO_2-brine-clay mineral particle system under geological CO_2 sequestration from subcritical to supercritical conditions, Chem. Eng. J. 347 (2018) 1-11.

[39] H. Ahn, M. Luberti, Z. Liu, S. Brandani. Process configuration studies of the amine capture process for coal-fired power plants, Int. J. Greenhouse Gas Control 16 (2013) 29-40.

[40] H.T. Oh, W.S. Lee, Y.S. Ju, C.H. Lee. Performance evaluation and carbon assessment of IGCC power plant with coal quality, Energy 188 (2019) 116063.

[41] I.V. Harbou, M. Imle, H. Hasse. Modeling and simulation of reactive absorption of CO_2 with MEA: Results for four different packings on two different scales, Chem. Eng. Sci. 105 (2014) 179-90.

[42] J.L. Bravo, J.A. Rocha, J.R. Fair. Mass-Transfer in Gauze Packings, Hydrocarbon Process. 64 (1985) 91-5.

[43] J. Stichlmair, J.L. Bravo, J.R. Fair. General model for prediction of pressure drop and capacity of countercurrent gas/liquid packed columns, Gas Sep. Purif. 3 (1989) 19-28.

[44] M. Afkhamipour, M. Mofarahi, A. Rezaei, R. Mahmoodi, C.H. Lee. Experimental and theoretical investigation of equilibrium absorption performance of CO_2 using a mixed 1-dimethylamino-2-propanol (1DMA2P) and monoethanolamine (MEA) solution, Fuel. 256 (2019) 115877.

[45] H. Hikita, S. Asai, H. Ishikawa, M. Honda. The kinetics of reactions of carbon dioxide with monoethanolamine, diethanolamine and triethanolamine by a rapid mixing method, Chem. Eng. J. 13 (1977) 7-12.

[46] Aspen Technology Inc. Aspen Physical Property Methods. Aspen Technology Inc., Cambridge, MA, USA, 2006.

[47] K.R. Putta, H.F. Svendsen, H.K. Knuutila. CO_2 absorption into loaded aqueous MEA solutions: Impact of different model parameter correlations and thermodynamic models on the absorption rate model predictions, Chem. Eng. J. 327 (2017) 868-80.

[48] R. Husan. The continuing importance of economies of scale in the automotive industry, Eur. Bus. Rev. 97 (1997) 38-42.

[49] C. Hendriks, W. Graus, F. van Bergen. Global carbon dioxide storage potential and costs. ECOFYS/TNO report EEP-02001, 2004.

[50] G. Towler, R. Sinnott. Chemical engineering design: principles, practice and economics of plant and process design, Second ed., Elsevier, Amsterdam, 2012.

[51] Aspen Technology Inc. Aspen Technology Guide, Aspen Technology Inc., Cambridge, MA, USA, 2009.

[52] Y.S. Jeong, J. Jung, U. Lee, C. Yang, C. Han. Techno-economic analysis of mechanical vapor recompression for process integration of post-combustion CO_2 capture with downstream compression, Chem. Eng. Res. Des. 104 (2015) 247-55.

[53] R. Ruegg, H. Marshall. Building economics: theory and practice, Springer Science & Business Media, Berlin, 2013.

Table list

Table 1. Literature review of process modifications of the strippers in CO_2 capture with amines [17, 18, 22-31].

	Author (year)	Solvent	Process modifications	Major Results
1	Dubois et al. [22] (2018)	MEA, PZ, PZ+MDEA	RSR, CSS, LVC, RVC	· Performance analysis and OPEX were evaluated for 3 amine solvents and 4 single configurations for the flue gas flow of 4000 m^3/hr. · All cases were optimized with the liquid-to-gas ratio to minimize energy consumption. · Performance analysis of CSS was conducted according to the cold flow split ratio. · Performance of LVC and RVC was optimized with a re-injection stage. · LVC was additionally analyzed with respect to pressure difference in a valve. · Minimum reboiler duty was to 2.39 GJ/tCO_2 from RVC using MDEA with PZ. · Minimum equivalent work was obtained from RSR using MEA.
2	Jiang et al. [18, 23] (2017, 2018)	NH_3 PZ+NH_3	Intercooling based CSS, CSS+advanced flash stripper	· Performance comparison for the variation of PZ concentration in reboiler duty was conducted for a 500 MW power plant. · Sensitivity analysis of the reboiler duty and equivalent work as a function of CO_2 lean loading and stripper pressure was performed. · Minimum reboiler duty was 1.97 GJ/tCO_2 when NH_3 with PZ was applied to CSS with advanced flash stripper.
3	Oh et al. [24, 25] (2016, 2018)	MEA	Pump-around, Multiple flue gas feed, Multiple lean solvent feed	· A superstructure-based optimization was conducted to minimize energy consumption and operating cost for CO_2 capture. · Sensitivity analysis of reboiler duty as a function of liquid-to-gas ratio and absorber inlet gas temperature was conducted. · The reboiler duty could approach to 3.36 GJ/tCO_2, and the operating cost could be reduced by 4.3% compared with the baseline configuration.
4	Zhao et al. [26] (2017)	PZ+MDEA	Intercooling, CSS, CSS+bypass, interheating	· Process analysis for a 650 MW power plant was conducted in terms of PZ concentration, absorption pressure, CO_2 removal ratio, and lean amine loading. · Performance was also analyzed according to intercooler position, cooling temperature and cold flow split ratio of CSS. · Reduction of reboiler heat duty from 2.74 GJ/tonCO_2 (baseline condition) to 2.24 GJ/tonCO_2 was achieved with developed configuration at optimum operating conditions.
5	Dutta et al. [17] (2017)	MEA	CSS, CSS+bypass,	· Dynamic simulation for performance analysis of the carbon capture process with a 600 MW natural gas power plant was conducted. · Two CCS-based configurations were analyzed, depending on flue gas flow rates at the

				full-load condition and assumed load variation of a power plant. · Sensitivity analysis of reboiler duty as a function of liquid-to-gas ratio, absorber pressure, and absorber inlet gas temperature was conducted. · Absorber diameter, one of the scale-up design factors at full-load condition, led to reducing reboiler duty.
6	Li et al. [27, 28] (2015, 2016)	NH_3	CSS, Interheating, CSS+bypass, CSS+interheating, CSS+bypass+interheating	· Techno-economic assessment was conducted for a 500 MW power plant. · Process analysis for NH_3 concentration, stripper pressure, split ratio, and lean amine loading was performed · Sensitivity analysis of operating cost as a function of individual utility cost was conducted. · Minimum reboiler duty was 2.46 GJ/tCO_2 in CSS with interheating configuration.
7	Li et al. [29] (2016)	MEA	Intercooling, CSS, CSS+bypass, interheating	· Techno-economic assessment was conducted for a 650 MW power plant. · Sensitivity analysis was conducted for reboiler duty, capital cost, CO_2 avoided cost, and levelised cost of electricity as a function of temperature difference in rich/lean amine heat exchanger. · Combined process configuration reduced reboiler duty from 4.0 to 3.08 GJ/tonCO_2.
8	Liang et al. [30] (2015)	MEA	CSS, SOC, SOC+CSS	· Performance analysis was conducted for a 300 MW power plant. · Detailed CSS with SOC configurations, split flow with vapor recompression process (SFVR) and improved split flow with vapor recompression process (ISFVR), were suggested. · Optimum conditions of liquid-to-gas ratio and cold flow split ratio were suggested. · Effects of stripper pressure on reboiler duty and equivalent work for a baseline process were evaluated. · Minimum reboiler duty was 1.676 GJ/tCO_2 in the configuration with ISFVR.
9	Jung et al. [31] (2015)	MEA	LVC, CSS, RVR, RVR+CSS, LVC+CSS	· A newly developed rich-vapor recompression (RVR) was suggested. · Economic analysis was conducted on all configurations in a 250-MW power plant after conducting performance and economic analysis for a 0.1 MW power plant. · Optimum values of split ratio or re-compressor outlet pressure were presented for all cases. · Minimum reboiler duty was 2.75 GJ/tCO_2 in RVR with CSS configuration.

Table 2. Operating conditions of the referenced process [35, 36] and the modified processes

Flue gas specification		**Rich amine specification**	
Temperature	49.07 □	Temperature	53.33 □
Pressure	1.1 bar	Pressure	1.09 bar
Flow rate	4974.92 Nm^3/hr	Flow rate	25104 kg/hr
CO_2 Mole fraction	0.11	CO_2 loading (mol/mol)	0.441
Lean amine specification		**Compressed CO_2**	
Temperature	40 □	Temperature	50 □
Pressure	2 bar	Pressure	152.7 bar
Flow rate	23948 kg/hr	Flow rate	24.95 kmol/hr
MEA concentration	30 wt.%	CO_2 recovery	90 %
CO_2 loading (mol/mol)	0.219	CO_2 mole fraction	99.9%
L/G ratio (mol/mol)	3.98		

Table 3. Specifications of the main units [35, 36, 42, 43]

Absorber specification	
Thermodynamic model	ENRTL-RK
Packing height	3 m[a] / 17 m
Packing diameter	1.1 m
Packing type	Sulzer Mellapak 2X
Top pressure	1.05 bar
Mass transfer coefficient method	Bravo et al.(1985) [34]
Interfacial area coefficient method	Bravo et al.(1985) [34]
Interfacial area factor	2.1
Heat transfer coefficient method	Chilton and Colburn
CO_2 removal efficiency	90 %
Hold up method	Stichlmair et al.(1989) [35]
Stripper specification	
Thermodynamic model	ENRTL-RK
Packing height	3 m / 10 m
Packing diameter	0.8 m / 1.1 m
Packing type	Sulzer Mellapak 2X
Top pressure	1.87 bar
Mass transfer coefficient method	Bravo et al.(1985) [34]
Interfacial area coefficient method	Bravo et al.(1985) [34]
Interfacial area factor	1
Heat transfer coefficient method	Chilton and Colburn
Hold up method	Stichlmair et al.(1989) [35]
Reboiler temperature	120 □
Heat exchanger specification	
Minimum temperature approach	5 □
Compressor & pump specification	
Efficiency	0.75

[a] For water washing section

Table 4. Performance assessment of reference and modified strippers under the optimum operating condition

Configuration	Splitter	Recompressor Vapor outlet pressure [bar]	Equivalent reboiler duty [kJ/mol CO_2]	Vapor recompression work [kJ/mol CO_2]	CO_2 compression work [kJ/mol CO_2]	Total equivalent work [kJ/mol CO_2]
Base	-	-	38.73	-	15.77	54.50
LVC	-	2	32.02	3.96	15.89	51.87
CSS	To HX 0.76	-	35.89	-	15.77	51.36
SOC 1	-	7.5	27.93	13.61	10.19	51.73
SOC 2	-	3.5	32.74	8.20	13.23	54.17
LVC + CSS	To HX 0.89	2	30.27	4.09	15.88	50.24
LVC + SOC	-	5.5	26.04	13.02	11.40	50.46
CSS + SOC	To HX 0.72	6.5	34.52	6.21	10.62	51.35
LVC + CSS + SOC	To HX 0.93	5.5	26.49	11.70	11.40	49.59

Table 5. Comparison of capital and operating costs among the modified carbon capture processes based on a 300-MW power plant

	Base	LVC	CSS	SOC 1	SOC 2	LVC+CSS	LVC+SOC	CSS+SOC	LVC+CSS +SOC
Capital Cost	198.05	247.23	189.24	229.41	228.93	245.64	278.43	196.21	264.30
Equipment cost	59.41	83.59	56.77	68.82	68.68	73.69	83.53	58.86	79.29
Absorber	21.86	21.86	21.86	21.86	21.86	21.86	21.86	21.86	21.86
Stripper tower	8.72	8.72	8.72	8.72	8.72	8.72	8.72	8.72	8.72
Compressor	18.14	34.18	18.14	26.15	26.01	33.67	42.86	20.36	38.73
Heat exchanger	9.85	8.06	7.23	11.25	11.23	8.10	8.75	7.08	8.65
Reboiler	0.45	0.42	0.42	0.43	0.44	0.42	0.42	0.43	0.42
Condenser	0.16	0.15	0.15	0.16	0.16	0.15	0.15	0.16	0.15
Flash vessel	-	0.52	-	-	-	0.51	0.51	-	0.51
Operating cost	55.30	52.05	51.54	51.63	54.42	50.31	50.42	51.57	49.68
Steam	37.60	31.17	34.60	27.10	32.33	29.45	25.31	33.57	25.80
Electricity	15.86	19.32	15.33	23.10	20.46	19.43	23.74	16.36	22.50
Cooling energy	1.84	1.56	1.61	1.43	1.63	1.43	1.37	1.64	1.38

* Capital cost unit: M$, Operating cost unit: M$/yr

Table 6. Comparison of cost savings based on assessment of a 300-MW power plant

Unit : M$	LVC	CSS	SOC 1	SOC 2	LVC+CSS	LVC+SOC	CSS+SOC	LVC+CSS +SOC
Capital cost change	49.18	-8.81	31.36	30.88	47.59	80.38	-1.84	66.25
Annual operating cost saving	3.25	3.76	3.67	0.88	4.99	4.88	3.73	5.62
Savings-to-Investment ratio	1.323	-	2.337	0.567	2.095	1.213	-	1.697

*project lifetime = 20 years

Figure list

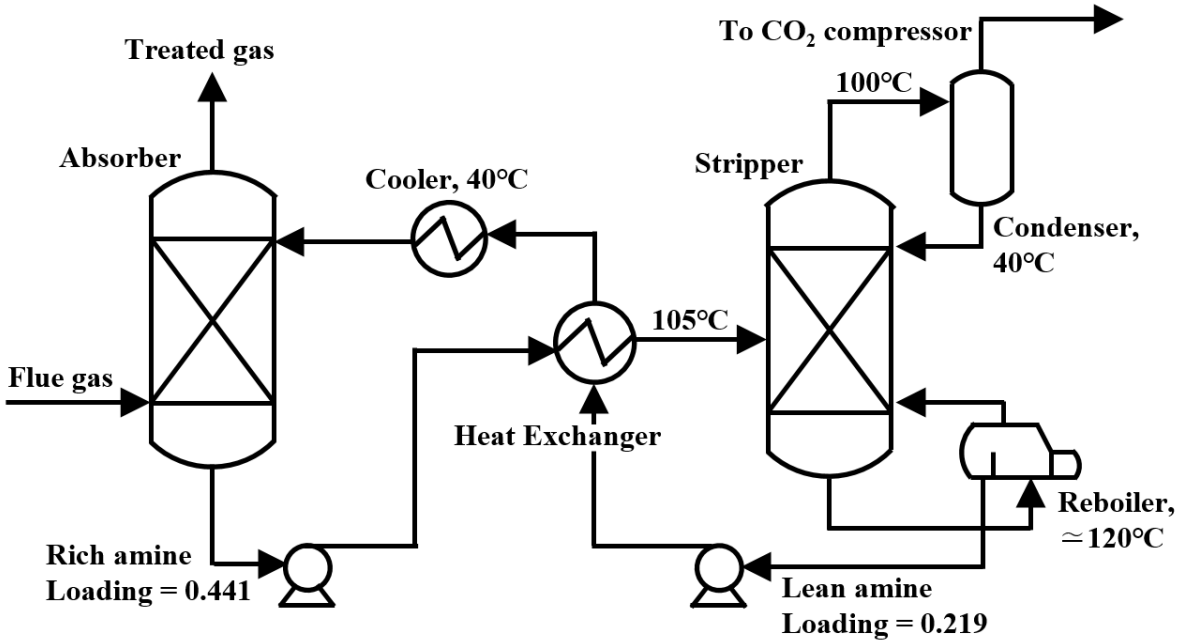

Fig. 1. A process flow diagram for the referenced MEA process [34, 35]

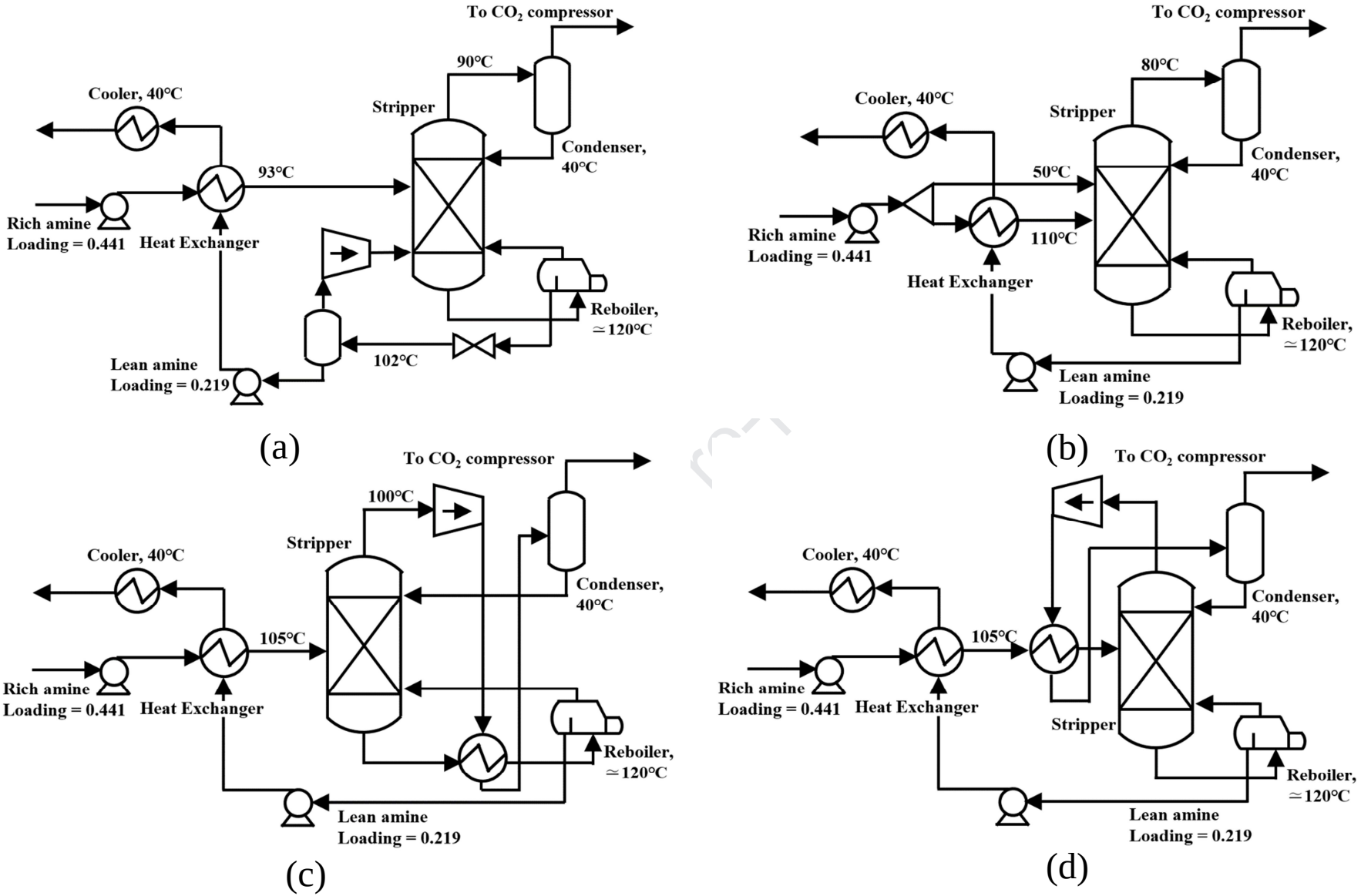

Fig. 2. A process flow diagram for alternative MEA processes [33-35]: (a) LVC, (b) CSS, (c) SOC case 1, and (d) SOC case 2

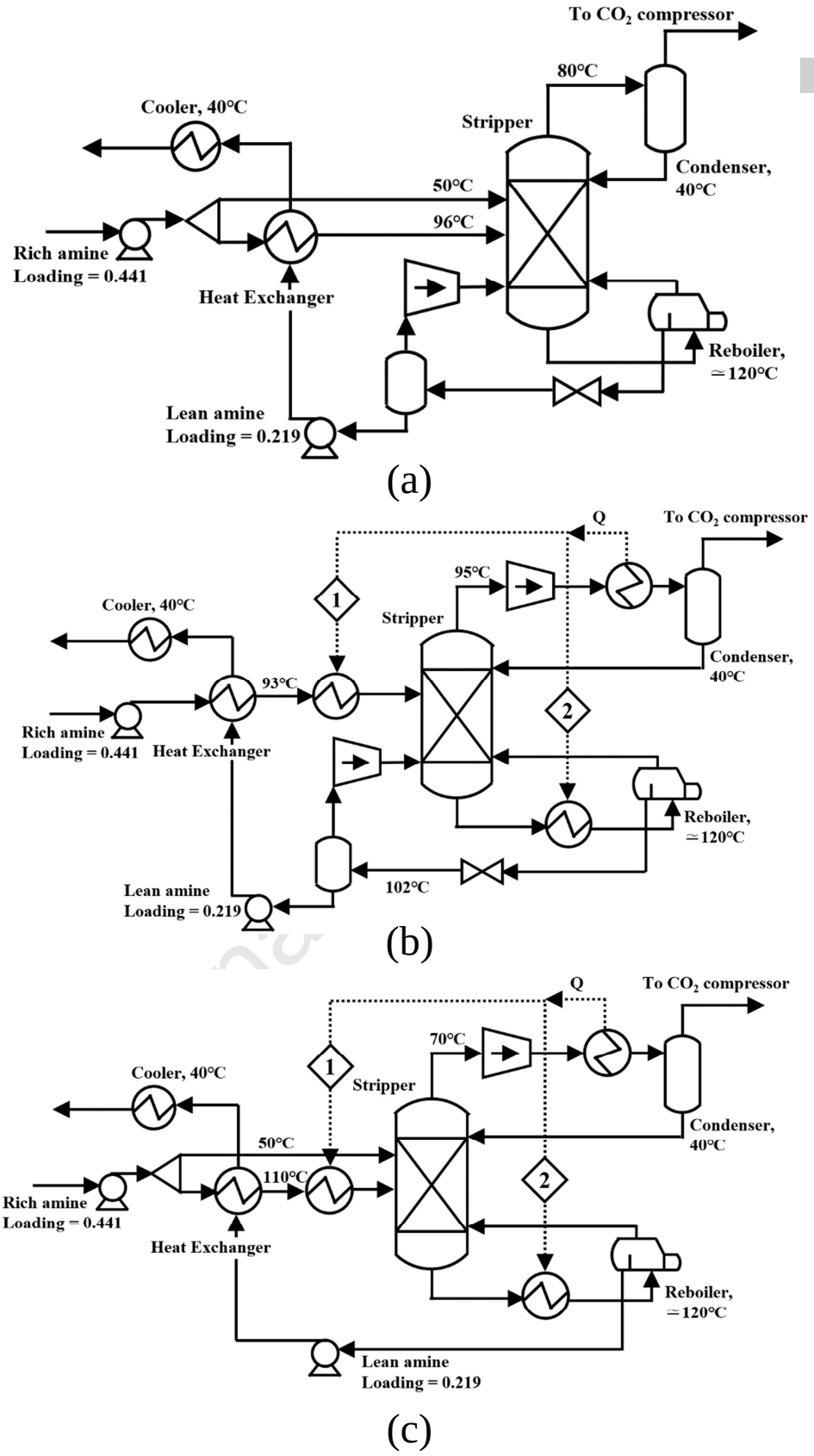

Fig. 3. Process flow diagrams for (a) LVC combined with CSS, (b) SOC combined with LVC, and (c) SOC combined with CSS.

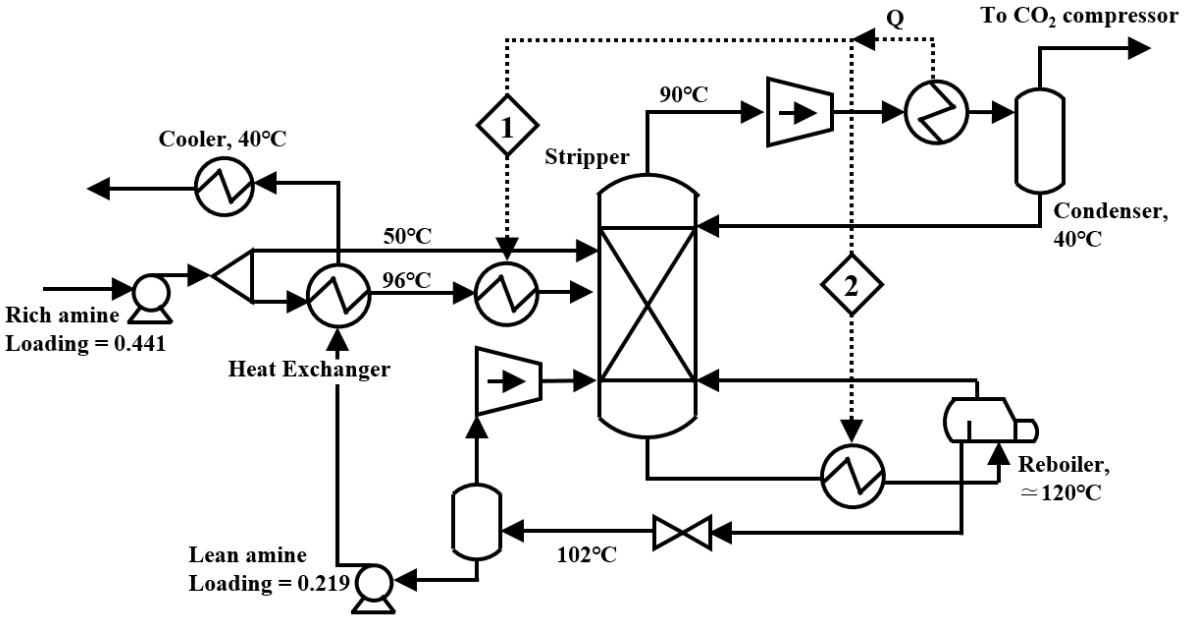

Fig. 4. A process flow diagram for SOC combined with LVC and CSS.

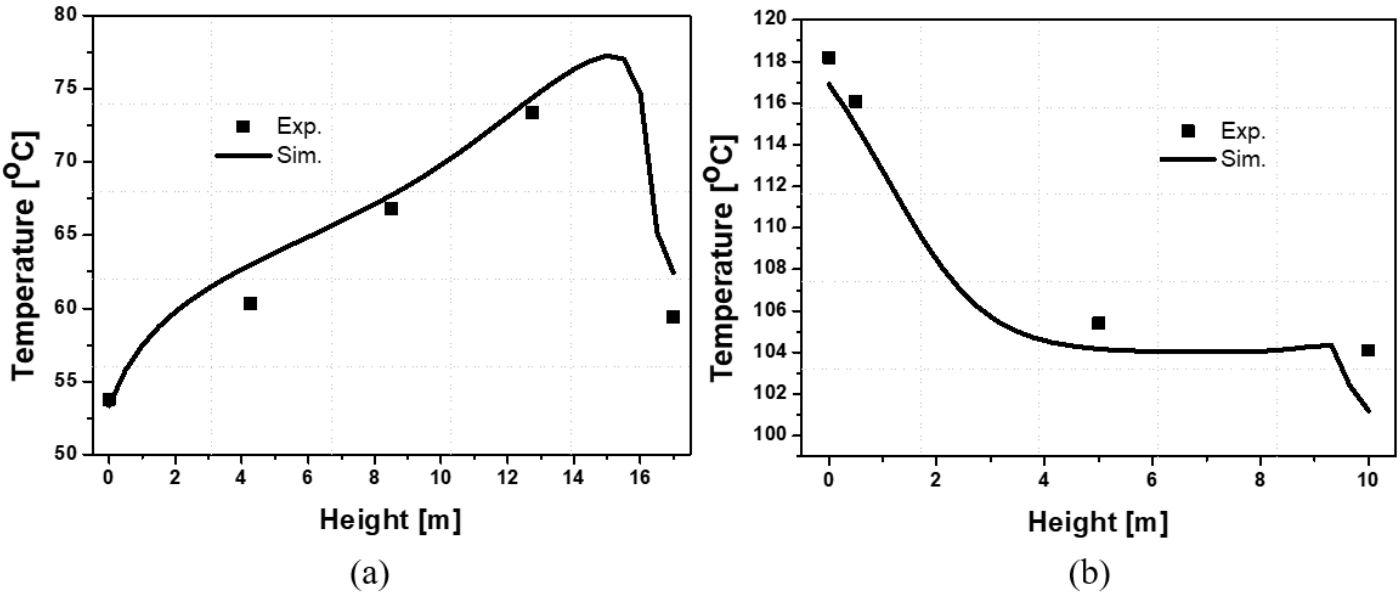

Fig. 5. Temperature profiles of experimental data [41] and simulation results for the reference process: (a) absorber and (b) stripper.

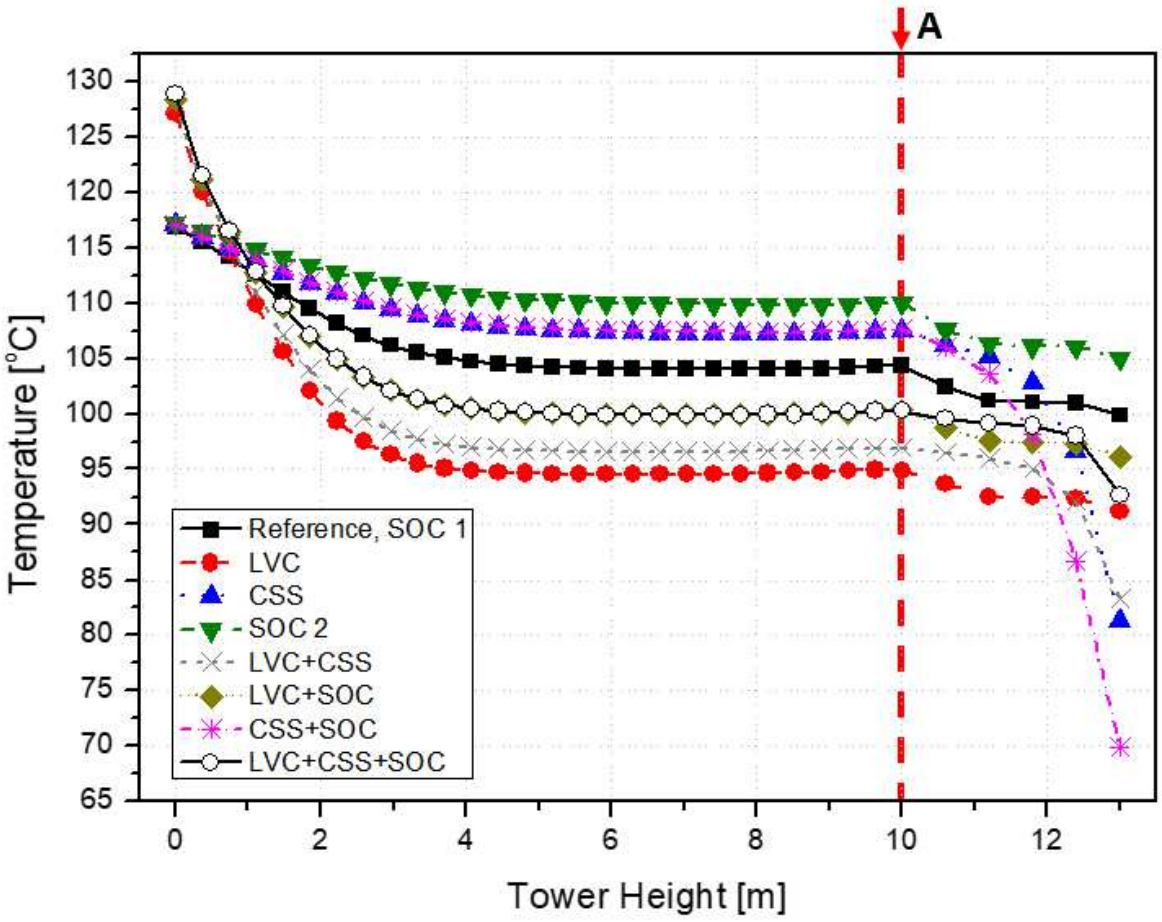

Fig. 6. Temperature profiles of the vapor phase in a stripper for all the cases under the optimum operating condition: "A" indicates the position of rich-solvent supply.

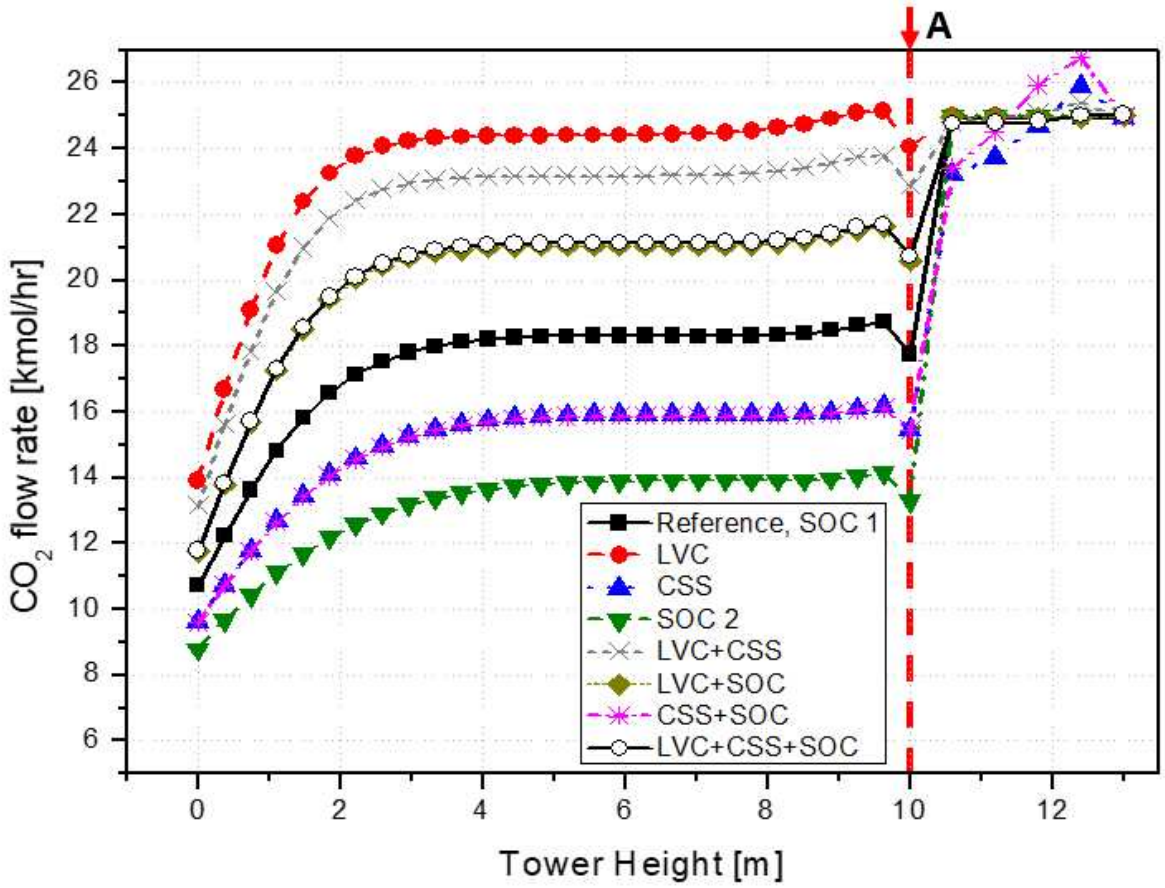

Fig. 7. Flow rate profiles of CO_2 in vapor phase in a stripper for all the cases under the optimum operating condition: "A" indicates the position of rich-solvent supply.

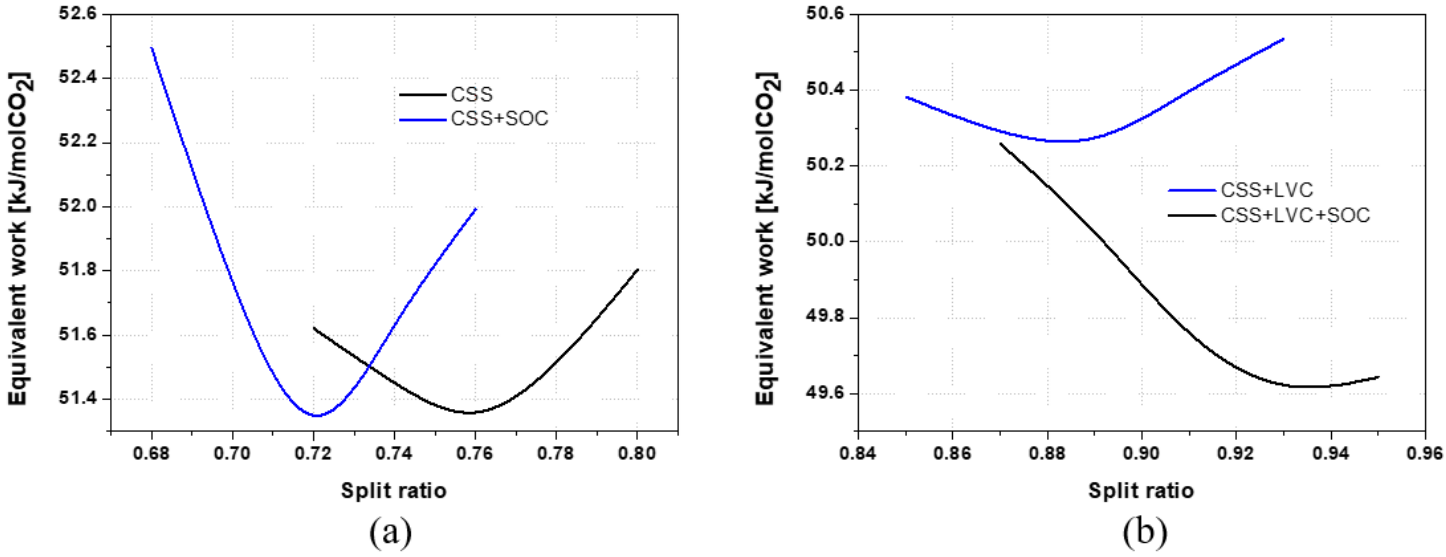

Fig. 8. Variation of equivalent work as a function of the split ratio: (a) CSS and CSS with SOC (b) LVC with CCS and SOC with LVC and CSS.

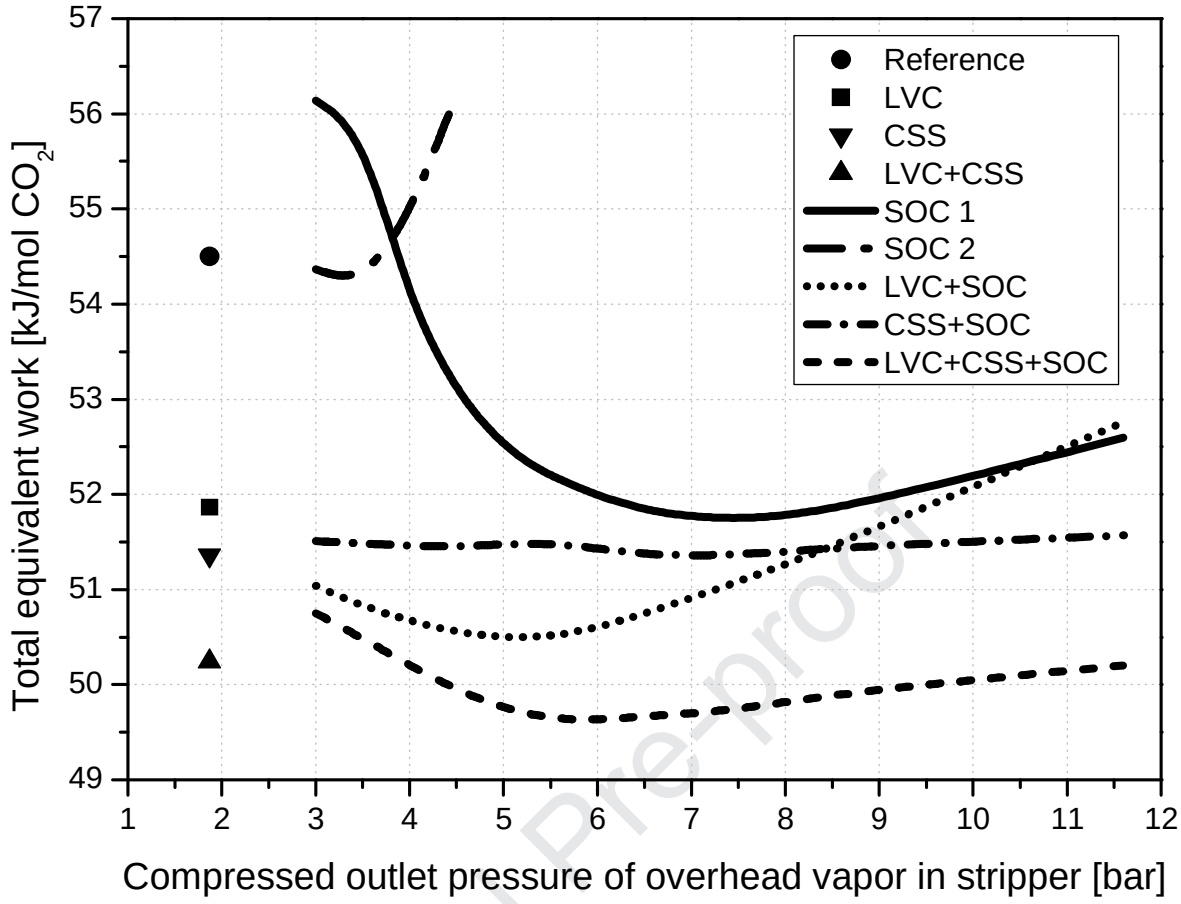

Fig. 9. Effect of compressed outlet pressure of the overhead vapor in a stripper on total equivalent work (Reference resulted from Tables 1 and 2, and Fig. 5).

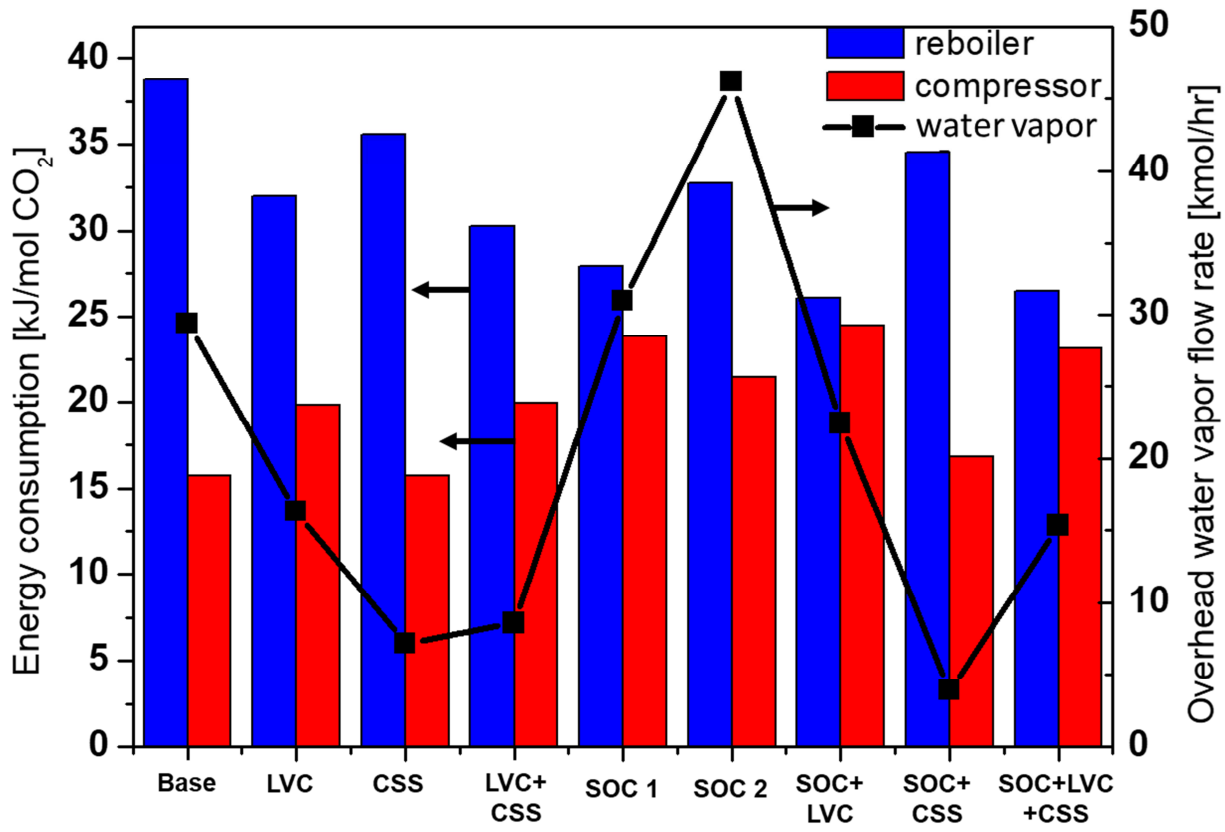

Fig. 10. Overhead water vapor flow rate and vapor compression energy/reboiler duty in a stripper at the optimum operating condition.

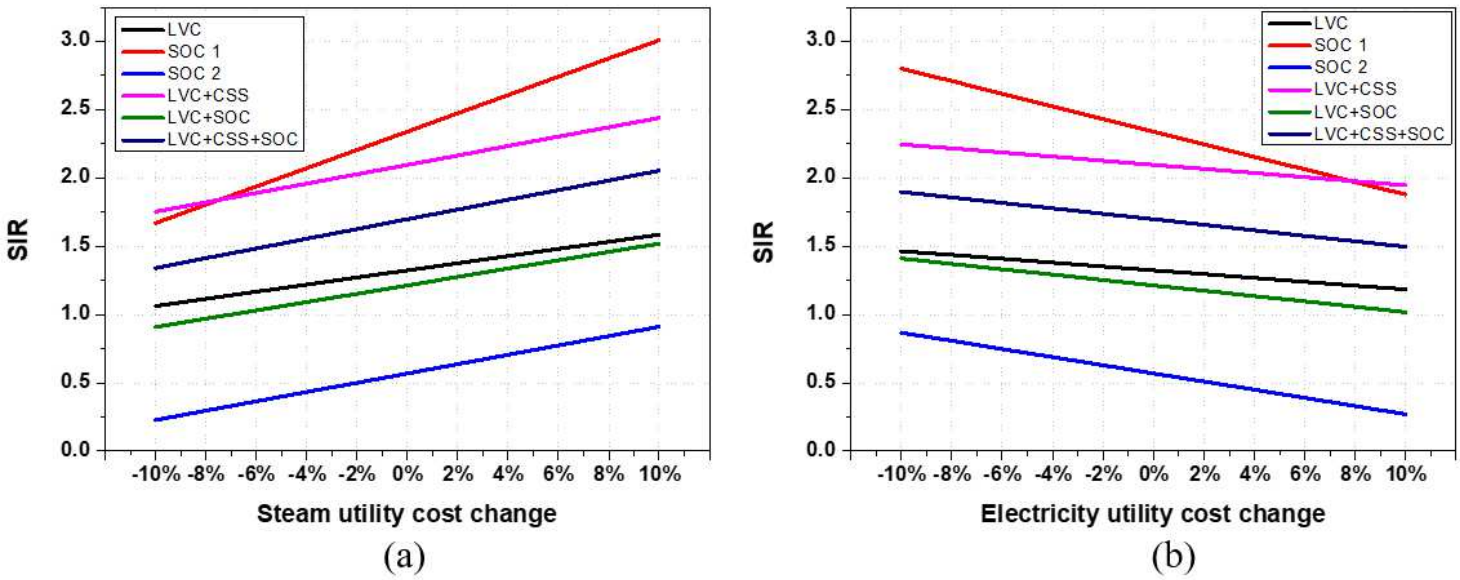

Fig. 11. Sensitivity analysis results for savings-to-investment ratio as a function of utility cost: (a) steam cost and (b) electricity cost

Highlights

- Techno-economic analysis of post-combustion carbon capture processes was conducted.
- Comparative analysis was performed on eight configurations of a 300-MW power plant.
- Strippers with two or more of LVC, CSS and SOC were developed to save energy.
- Total equivalent work was saved by 9.0% and operational expenditure by 10.2%.
- In terms of SIR, developed processes can be alternative to the conventional process.

Declaration of interests

☒ The authors declare that they have no known competing financial interests or personal relationships that could have appeared to influence the work reported in this paper.

☐The authors declare the following financial interests/personal relationships which may be considered as potential competing interests: